Natural Resources Canada
Ressources naturelles Canada

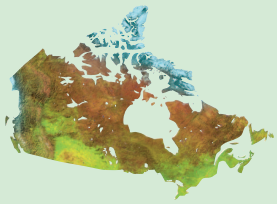

Uranium-rich bostonite-carbonatite dykes in Nunavut: recent observations

T.D. Peterson, J.M.J. Scott, and C.W. Jefferson

Geological Survey of Canada

Current Research 2011-11

2011

Canada

Geological Survey of Canada
Current Research 2011-11

Uranium-rich bostonite-carbonatite dykes in Nunavut: recent observations

T.D. Peterson, J.M.J. Scott, and C.W. Jefferson

2011

ISSN 1701-4387
Catalogue No. M44-2011/11E-PDF
ISBN 978-1-100-18908-6
doi:10.4095/288751

A copy of this publication is also available for reference in depository libraries across Canada through access to the Depository Services Program's Web site at http://dsp-psd.pwgsc.gc.ca

A free digital download of this publication is available from GeoPub: http://geopub.nrcan.gc.ca/index_e.php

Toll-free (Canada and U.S.A.): 1-888-252-4301

Recommended citation

Peterson, T.D., Scott, J.M.J., and Jefferson, C.W., 2011. Uranium-rich bostonite-carbonatite dykes in Nunavut: recent observations; Geological Survey of Canada, Current Research 2011-11, 12 p. doi: 10.4095/288751

Critical review

E. Potter

Authors

T.D. Peterson (Tony.Peterson@NRCan-RNCan.gc.ca)
J.M.J. Scott (Jeffrey.Scott@NRCan-RNCan.gc.ca)
C.W. Jefferson (Charlie.Jefferson@NRCan-RNCan.gc.ca)
Geological Survey of Canada
601 Booth Street
Ottawa, Ontario
K1A 0E8

Correction date:

Uranium-rich bostonite-carbonatite dykes in Nunavut: recent observations

T.D. Peterson, J.M.J. Scott, and C.W. Jefferson

Peterson, T.D., Scott, J.M.J., and Jefferson, C.W., 2011. Uranium-rich bostonite-carbonatite dykes in Nunavut: recent observations; Geological Survey of Canada, Current Research 2011-11, 12 p. doi: 10.4095/288751

Abstract: Anomalously radioactive dykes near Deep Rose Lake (NTS 66 G/8) consist of potassic microsyenite (bostonite) with and without carbonate-rich portions. One dyke-like body consisting of carbonate alone (+ minor chlorite) was also found. Radiation measurements of up to 9000 counts per second (equivalent uranium (eU) = 519 ppm, equivalent thorium (eTh) = 34 ppm) in outcrop result from concentrations of uranium silicates, uranium-thorium oxides, and monazite. One carbonate-rich dyke also contains a REE-bearing carbonate phase. The syenites are interpreted as coming from strongly differentiated ultrapotassic magma related to the Dubawnt minette suite (ca. 1.83 Ga), and the carbonate as a product of further igneous differentiation (carbonatite). Anomalously radioactive and REE-rich bostonite dykes and small plutons related to the Dubawnt minettes are broadly distributed from latitude 60° to at least as far north as the Amer mylonite zone.

Résumé : Des dykes situés près du lac Deep Rose (SNRC 66 G/8), qui montrent des anomalies radioactives, sont constitués de microsyénite potassique (bostonite) avec ou sans parties riches en carbonates. Une masse en forme de dyke constituée seulement de carbonate (avec de petites quantités de chlorite) a également été trouvée. Des niveaux de rayonnement gamma allant jusqu'à 9000 coups par seconde (équivalent uranium (éU) = 519 ppm, équivalent thorium (éTh) = 34 ppm) ont été mesurés sur les affleurements; ce rayonnement est fonction des concentrations de silicates d'uranium, d'oxydes d'uranium et de thorium, et de monazite. Un dyke riche en carbonates renferme également une phase carbonatée contenant des terres rares. Selon notre interprétation, les syénites seraient issues de magma ultrapotassique fortement différencié, apparenté à la suite de minettes de Dubawnt (vers 1,83 Ga), et le carbonate serait le produit d'une différenciation ignée plus poussée (carbonatite). Des dykes de bostonite et de petits plutons, à radioactivité anomale et riches en terres rares, apparentés aux minettes de Dubawnt, sont très répandus depuis 60° de latitude nord jusqu'à la zone de mylonite d'Amer, et peut-être même plus au nord.

INTRODUCTION

Numerous occurrences of uranium, thorium, and REE-rich rocks related to igneous activity within the Dubawnt Supergroup (ca. 1.85–1.55 Ga) have been noted (e.g. Miller, 1980; LeCheminant et al., 1987). Some are associated with hydrothermally generated metalliferous veins (particularly silver-copper-bearing veins), but the richest uranium-thorium-REE occurrences are hosted by strongly potassic intrusive suites that have been correlated with the phlogopite-rich lavas of the Christopher Island Formation and its feeder dykes (mainly of minette composition). These intrusive suites include the Enekatcha intrusion (NTS 65 E/15: Miller and Blackwell, 1992) and a swarm of fine-grained, biotite-bearing felsite (bostonite) dykes in the area southwest of Baker Lake (Miller, 1979; LeCheminant et al., 1987) (Fig. 1). Hereafter we will refer to these rocks as the Dubawnt minettes (Peterson et al., 2002).

In the course of 2010 field studies on Dubawnt-aged granitic intrusions in the Deep Rose Lake area (NTS 66 G/8), two occurrences of anomalously radioactive rocks (up to 9000 counts per second gamma-ray emissions; eU = 519, eTh = 34 ppm), 1.5 km apart, were located in outcrop (Fig. 1). One of the occurrences also features a 1 m wide, fine-grained, anomalously radioactive boulder situated on top of the outcrop. Texturally and mineralogically, these rocks closely resemble the felsite dykes described by LeCheminant et al. (1987).

Because the showings contain significant coarse carbonate, enigmatic black schistose bands and other components that are too fine-grained for field identification, it was initially uncertain whether the elevated uranium-thorium is the result of relatively low-grade hydrothermal alteration or is an integral part of the igneous suite. Furthermore, interpretation of the most radioactive outcrop (J34) was hindered by lichen and soil cover. Subsequent examination in thin section revealed that much of the anomalously radioactive material is a very fine-grained igneous intrusion, essentially identical to a moderately radioactive bostonite dyke intruding quartzite of the Amer Group, sampled 6.3 km south-southwest of the anomalous outcrops. These occurrences are summarized in Table 1.

The outcrops are scattered over an approximately 21 km^2 area 12.5 km south of the Amer Fault Zone (Fig. 1). About 5% of the outcrop exposures are clustered beside unusually large, coarse, and steep-walled eskers with numerous kettle lakes. The geology of the area features early Paleoproterozoic quartzite of the Amer Group that unconformably overlies Neoarchean mafic volcanic and silicic plutonic rocks. The Paleoproterozoic and Neoarchean rocks were multiply deformed, structurally intercalated, and transected by early ductile stages of Amer Mylonite Zone (AMZ) before intrusion of late Paleoproterozoic stocks and brittle right-lateral reactivation of the AMZ (Tella et al., 1983; Tella, 1994; Tella et al., unpub. rept., 2011). North of the AMZ, the exposed granite is coarse grained, rapakivi textured, and appears to be uniformly part of the ca. 1750 Ma Nueltin Suite (Peterson et al., 2002). South of the fault, a single U-Pb (zircon) age of 1850 +30/-10 Ma (Tella et al., 1985) and the nonporphyritic, heterogeneous (mixed magma) characteristics indicate that much of the exposed granite is part of the regionally extensive Hudson granitoid suite (van Breemen et al., 2005). However, some coarse-grained granite with a mineralogy similar to the north-side Nueltin granite was noted; characterization of these granitoid suites is in progress (Scott et al., unpub. rept., 2011).

FIELD DESCRIPTIONS

Gamma-ray responses were measured in the field using calibrated RS-230 portable spectrometers manufactured by Radiation Solutions Inc. Outcrop exploration and mapping were done in survey mode, with gamma-ray emissions measured in counts per second (cps). Equivalent uranium (eU), equivalent thorium (eTh) and potassium (K) contents were measured on flat outcrop surfaces using a 120 s assay mode.

PHA10-J34A: radioactive bostonite-carbonate

The host rock for this occurrence is heterogeneous granodiorite-granite, containing wispy patches of dioritic material on a scale of 5 cm to 1 m, interpreted to be a result of mingling of mafic and granitic magmas (Fig. 2a). The outcrop lacks a penetrative deformation fabric and neither discrete faults nor shear zones were noted. The uranium-rich rocks identified by gamma-ray spectrometry form a 340° trending tabular body on the eastern edge of the granodiorite outcrop. The anomalous zone, about 10 cm wide, is only exposed for about 1 m due to till cover . Gamma-ray spectrometer counts of up to 9000 cps were recorded on flat surfaces, with a eU/eTh ratio of 15 (eU/eTh = 519/34 ppm).

The tabular rock body consists of fine-grained, schistose and greasy-lustred to flinty black and cherty red rock. The black material contained irregular and discontinuous patches of pale, coarse carbonate (Fig. 2b). Samples were collected by hammer and chisel, as chips and small, flat hand specimens, then packaged in sealed plastic bags. A 'reconstruction' of this occurrence, based on thin section and scanning electron microscope (SEM) study (below), indicates that the black carbonate-rich portion occupies a central zone, flanked by cherty rock that is brecciated and veined by the carbonate material.

PHA10-J34B: radioactive bostonite

Anomalous radioactivity was noted in a well rounded and subspherical boulder approximately 1 m in diameter situated on top of outcrop J34A. The maximum gamma-ray response detected in the flinty, tan- to ochre-weathering boulder was

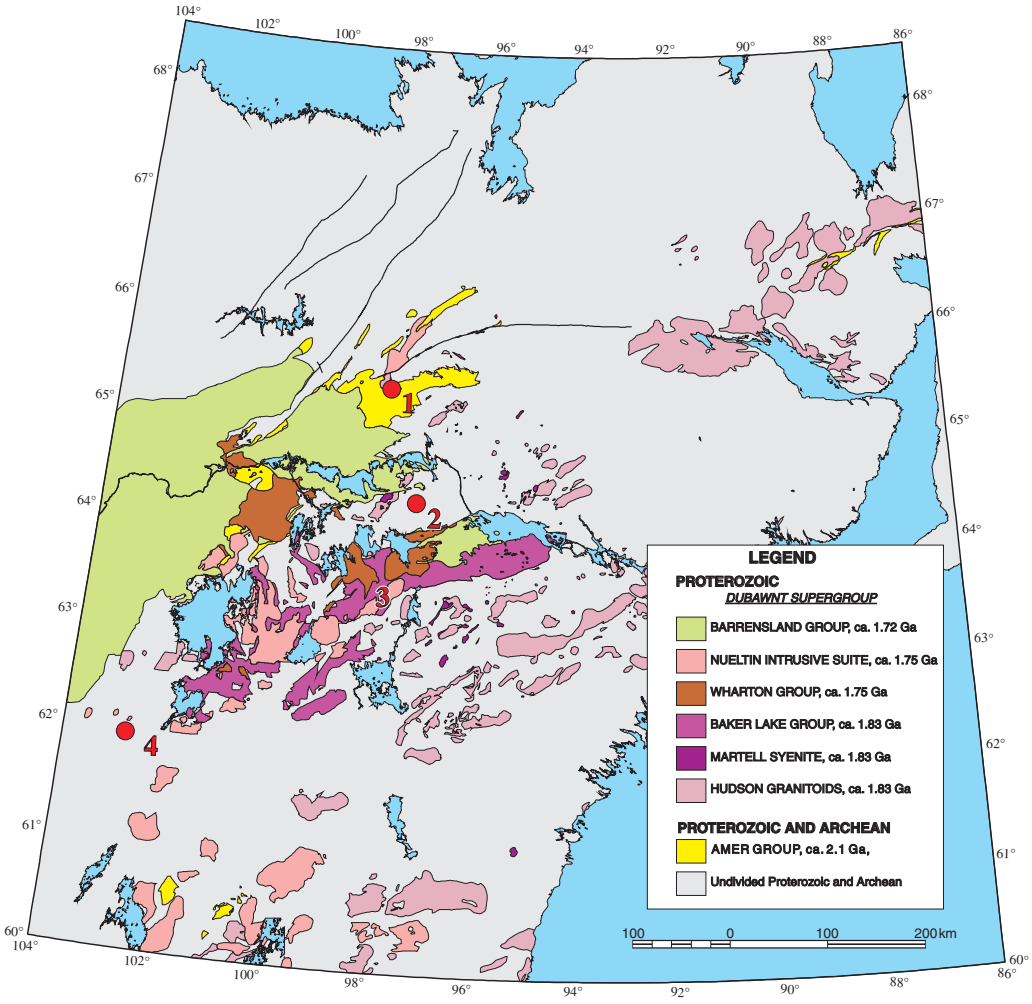

Figure 1. Locations of the areas discussed in the text. 1 (circle): J34, J37, and J45; 2 (circle): Judge Sissons pluton; 3: general area containing bostonite dykes; 4 (circle): Enekatcha Lake.

Table 1. Occurrences discussed in this paper.

Sample	Form	Rock type	cps	U	Th	Lat.	Long.	Map unit*
PHA10-J34A	outcrop	felsite/carbonatite	8950	519.4	34.1	65.4006	-98.1410	PDR
PHA10-J34B	boulder	felsite/carbonatite	3800	239	22.6	65.4006	-98.1410	PDR
PHA10-J37	outcrop	carbonatite	850	58.7	3.1	65.3966	-98.1746	PDR
PHA10-J42	subcrop	granite	700	13.7	53.2	65.3830	-98.2281	PDH
PHA10-J045	outcrop	felsite dyke	NA	NA	NA	65.3482	-98.0905	PDR
JP08-62	outcrop	quartz syenite	Unknown					PDM

* PD-Proterozoic/Dubawnt, R-Rose bostonite/carbonatite dykes (new unit), H-Hudson granitoid suite, M-Martell syenite suite.
NA-not analyzed

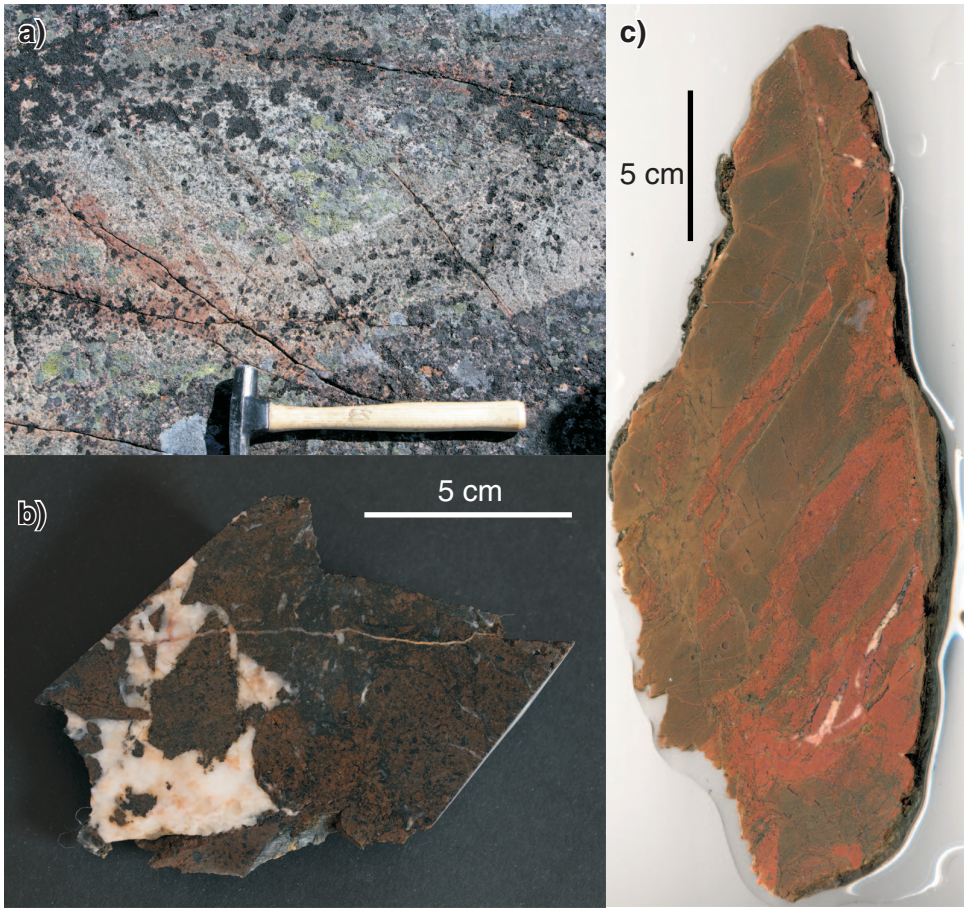

Figure 2. a) Mingled granodiorite-diorite, host to occurrence PHA10-J34A. Photograph by J. Scott. 2011-028A. **b)** Sawn surface showing white carbonatite within bostonite, sample J34a. Photograph by T. Peterson. 2011-028B. **c)** Cherty bostonite, occurrence J34b (boulder). The red bands consist of brecciated quartz + hematite (*see* text). Photograph by T. Peterson. 2011-028C

4000 cps with eU/eTh = 10 (239/23 ppm). A collection of shards was obtained with difficulty from an area near the portion of highest radioactivity (Fig. 2c). The boulder resembled the red, cherty portion of J34A. Numerous boulders of similar appearance have been reported by prospecting teams of different companies in this region since the 1980s. These are thought to be glacial erratics with local provenance.

PHA10-J37: radioactive carbonate

The host rock of this occurrence is a medium-grained, blue-black gabbro (quartz-bearing amphibolite), locally rich in brassy sulphide minerals. The outcrop is isolated, occurs within an area of white Amer Group quartzite, and is approximately 100 m in length. There are numerous inclusions of quartzite in the gabbro, but the outer contacts are not exposed. The outcrop is undeformed, except for a discrete band of schistose material (subvertical and trending 050°) that crosses near the high point of the outcrop (Fig. 3a). The schistose zone is occupied over a length of about 20 cm by coarse carbonate, with a prominent caliche covering, which gave gamma-ray counts up to 850 cps, with eU/eTh = 20 (59/3 ppm). The carbonate was heterogeneously coloured in white, red, and green (Fig. 3b). Two 10 cm long hand samples (10PHA-J37) were collected by hammer and chisel.

PHA10-J45: bostonite dyke

This station is located 6.3 km south of station J34, on ground held by a Titan Uranium – Mega Uranium Joint Venture. The host rock for this occurrence is clean, white quartzite of the Amer Group. A pale pink- to orange-weathering felsite (bostonite) dyke, trending 290/75, is exposed along a cliff face at the top of which is an abandoned falcon nest. As only one contact is exposed, its thickness is uncertain; however the northwesterly continuation of this dyke, as evidenced by frost boils in till, has a maximum width on the order of 2 to 3 m. The dyke material is homogeneous and shows no local coarsening or variation in mineralogy. It is moderately radioactive with a gamma ray response of 500 to 700 cps. When hammered, it was noticed that the dyke consistently broke into relatively regular, flaggy blocks which are lined with iron oxide.

PETROGRAPHY AND MINERALOGY OF THE OCCURRENCES

Thin sections and small pieces of samples were studied using petrographic and scanning electron microscopes (SEM).

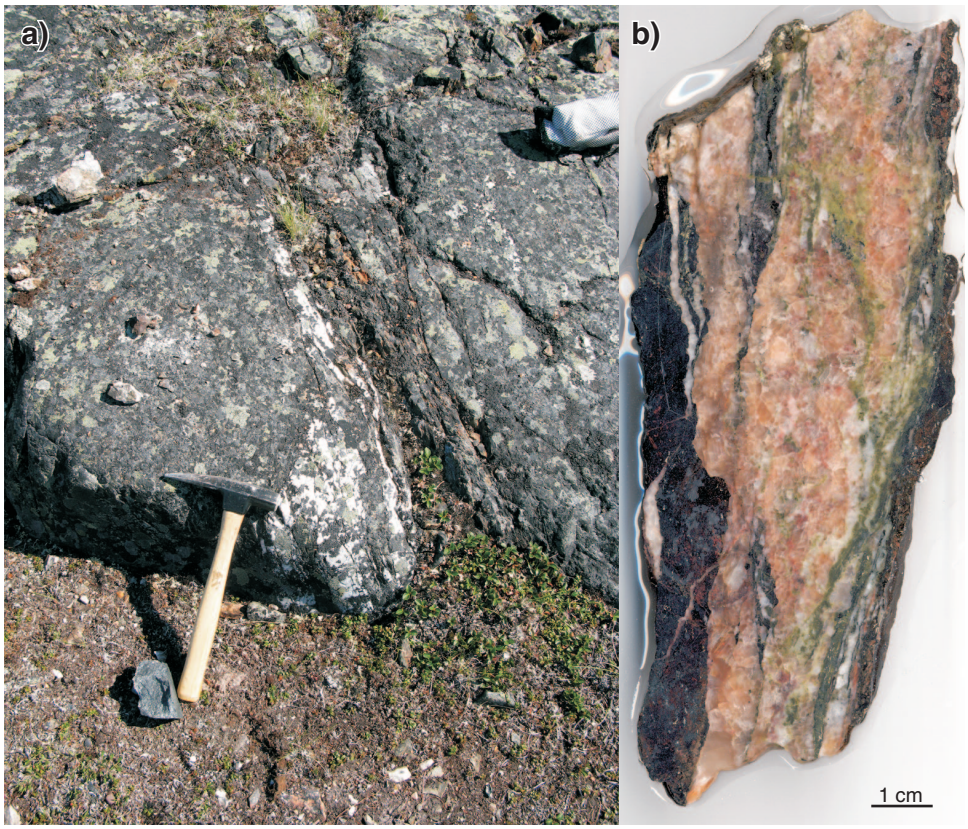

Figure 3. a) Outcrop at station J37, showing the foliated band containing the anomalously radioactive carbonate. Note the white patch of Amer quartzite next to the hammer, included in the host intrusion which is a dark gabbro rich in sulphides. 2011-031A. **b)** Hand sample of the carbonatite, J37. The black band on the left is a portion of the host gabbro, with some carbonate veining. The green chlorite wisps are rich in monazite. 2011-031B. Photographs by J. Scott.

PHA10-J34A: bostonite-carbonate

There are two lithological components in the occurrence: bostonite (fine-grained potassic syenite) and carbonate-rich material. The bostonite consists of very fine-grained potassic alkali feldspar with subordinate, calcium-poor plagioclase, and minor biotite (mostly chloritized) plus magnetite (Fig. 4a, b). The bostonite is rich in carbonate patches, ranging from 2 to 3 mm to microscopic in size and which have clearly defined contacts with the bostonite minerals. Replacement textures (e.g. calcite after plagioclase) were not noted. In most cases, the carbonate fills angular interstitial spaces between silicate minerals, forming an intercumulate texture. The bostonite is also extensively veined and brecciated by coarse calcite + iron chlorite (Fig. 4c). Apatite, monazite, and zircon are prominent accessory phases.

The carbonatite is heterogeneous. Thin veins in the bostonite, separate from the main carbonatite body, consist of calcite+hematite+magnetite+apatite+quartz (Fig. 4d); specific uranium-thorium-bearing minerals were not observed. Galena, chalcopyrite, and native bismuth are present. The quartz is often rich in a sodium-rich pyribole, likely aegirine, present in needles 2 microns wide. Hematite forms clusters of needles and blades, up to 3 mm long, that are steel blue on thin edges and that appear to be primary, although minor secondary red hematite is also present.

The highly radioactive fragments were not studied in thin section but rather as centimetre-scale pieces under the SEM. The pieces contain discrete veins and botryoidal masses of uranium+lead oxides (Fig. 5a, b, c) within fine-grained carbonate, plus finely disseminated UO_x. Grains of calcite contain discrete crystals and subspherical aggregates of a uranium-silicon-calcium mineral (Fig. 5d, e); energy-dispersive X-ray spectra (EDS spectra) are consistent with uranophane. Thin fracture planes coated with light rare-earth-element carbonates crosscut the calcite (Fig. 5a, f).

Some of the margins of the studied carbonate pieces, which have a greasy micaceous lustre, are dominated by iron-rich chlorite that represents the contact zone between the carbonate and bostonite phases, and is the mineral responsible for the schistose fabric in some portions of the outcrop. The composition of this chlorite is similar to that present in the carbonate-chlorite breccia zones within the bostonite.

PHA10-J34B: radioactive bostonite boulder

In thin section, this sample is a homogeneous bostonite containing planes rich in angular, broken quartz grains with deformation features (strain shadows, fluid inclusion trains) set in a hematite-rich matrix (Fig. 2d). Thicker (centimetre-scale) planes have sharp contacts, but thin (millimetre-scale) ones have gradational contacts with the enclosing felsite. Both types, but particularly the thinner planes, were plastically

deformed along with the felsite. They are interpreted as microbrecciated, fluidized host Amer quartzite which was injected into the felsite dyke before it completely solidified.

This sample is very similar to the syenite portion of J34a, but carbonate is not present. Specific U-Th-REE minerals were not noted, but the felsite is very rich in monazite (with lesser zircon); this monazite is presumably the source of the boulder's radioactivity.

PHA10-J37: radioactive carbonate

The carbonate portion of this sample (grain size up to 1 cm) is relatively pure, except for minor disseminated galena + chalcopyrite. The green and red hues (Fig. 3b) are from minor hematite and chlorite + epidote. An SEM study of the caliche coating on the outcrop revealed no radioactive minerals were present within it.

The radioactive portions of this occurrence appear to be chlorite-rich bands, with characteristics intermediate between those of J34a and J34b. They contain well formed tabular to irregular crystals of calcite, and are extremely rich in monazite crystals about 30 microns in diameter. Coarse yellow-green epidote crystals occur within and adjacent to the chlorite. There are no portions of this sample that have any deformational features, and the foliation observed in outcrop is due to alignment of chlorite parallel to the carbonate dyke walls, and recrystallization of the gabbro.

PHA10-J45: bostonite dyke

The sample is a fine-grained microsyenite which consists of subequal amounts of plagioclase microphenocrysts (completely replaced by white micas) in a groundmass of reddish, mostly unaltered potassium feldspar. Minor phlogopite

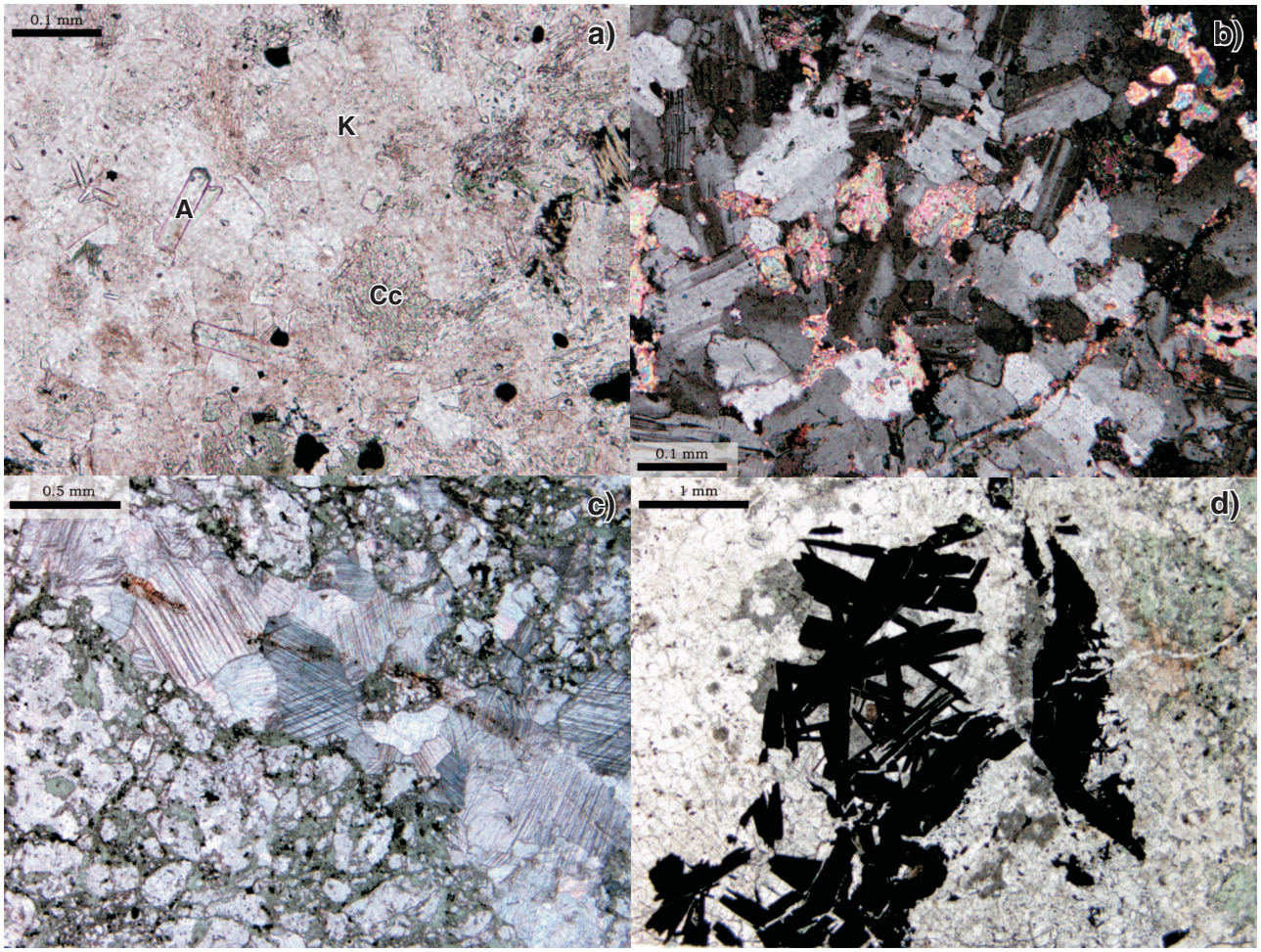

Figure 4. Photomicrographs of the bostonite/carbonatite J34a. **a)** Bostonite (microsyenite portion), plane-polarized light. A = apatite, K = potassium feldspar, Cc = carbonate. Black magnetite, altered biotite (left edge), and green Fe-rich chlorite (bottom edge) are present. 2011-030A. **b)** Bostonite, crossed polars. Note the large quantity of highly birefringent interstitial carbonate, which has not replaced any other mineral. 2011-030B. **c)** Vein of calcite in bostonite, which is brecciated by green Fe-rich chlorite + carbonate (partially crossed polars). 2011-030C. **d)** Large primary hematite crystals in a distal carbonate vein in the bostonite. The white areas are quartz + apatite; subordinate carbonate forms the darker areas adjacent to the hematite. Green is Fe-rich chlorite. 2011-030D. Photographs by T. Peterson.

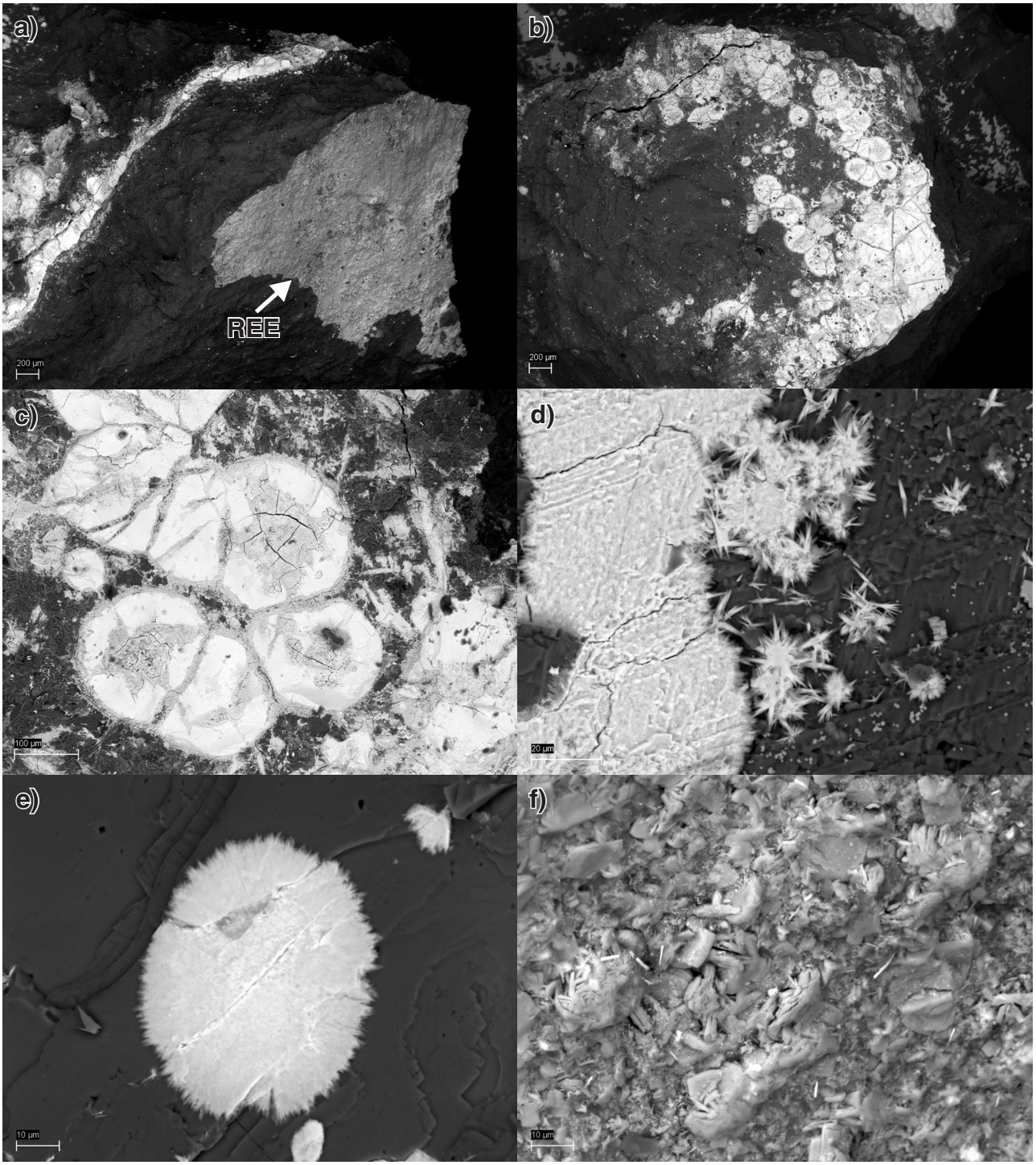

Figure 5. Backscattered electron images of one piece of the carbonate-rich material in sample J34a. 2011-027A. **a)** Bright vein of U-Pb oxides in dark carbonate. The area labelled REE is a thin surface coated with carbonates of LREE, mainly La and Ce. **b)** Spherical (botryoidal) concentrations of U-Pb oxide. 2011-027B. **c)** Close-up of b). **d)** Acicular crystals of a U-Si-Ca mineral (uranophane?) in coarse calcite. 2011-027D. **e)** Spherical aggregate of uranophane (?) in calcite. 2011-027E. **f)** Detail of the REE carbonate surface in image a). 2011-027F. Photographs by P. Hunt.

microphenocrysts are typically contorted. Millimetre-scale patches of green-brown chlorite may be secondary after clinopyroxene, and minor hematized magnetite(?) is present. The groundmass contains clear, euhedral microphenocrysts of apatite and is rich in extremely fine-grained, dusty to framboidal monazite, which may in part be intergrown with zircon. Quartz veins, up to 4 mm wide, cut the sample.

GEOCHEMISTRY

Samples were analyzed by ALS Minerals (Vancouver). The samples from sites J34 and J37 were pulverized using an agate mill and analyzed by a fusion inductively coupled plasma mass spectroscopy (ICP-MS) technique (ME-MS81u) for trace elements, a four-acid inductively coupled plasma atomic-emission spectroscopy (ICP-AES) technique (ME-ICP61a) for base metals, ion electrode for F (F-ELE81a), and neutron activation analysis (NAA) for Cl (Cl^-NAA06). Sample J45 was characterized by combined X-ray fluorescence and ICP-mass spectrometry (package 4X4B) with F analyzed by ion electrolyte (2A04) and FeO by titration (G806). Five aliquots of approximately 5 g were selected from J34A in an effort to isolate the most radioactive portion of the sample. The results are given in Table 2.

Uranium contents were exceptionally high in only one sample, aliquot 00 from J34A, which came from the same part of the sample where UO_x and uranophane were located. This portion has very high U/Th values (U/Th = 368) but the other portions have U/Th values averaging 1. The U-rich portion also had the highest rare-earth element (REE) contents (Ce = 265 ppm) and unusually high Y (84 ppm) and Cu (450 ppm). Lead in this portion is also very high (2440 ppm), and is clearly associated with U through radioactive decay.

The U/Th values are moderately high in the bostonite boulder J34B (U/Th = 15.8) and very high in both carbonate samples from J37 (average 700) with moderate U contents (average 360 ppm). Rare-earth element concentrations are very low in the J37 analyses. The bostonite dyke J45 has U contents comparable to the U-poor portions of J34A (17 ppm) and low U/Th (0.55) but REE contents comparable to the U-rich portion (Ce = 246 ppm).

The trace-element concentrations of these rocks are compared to other rocks of the Dubawnt Supergroup in Figures 6a) and b). The 'Enekatcha shonkinite' is an average of 12 analyses (Peterson, unpub. data) of samples collected by A. Miller near Enekatcha Lake (NTS 65 E/15) (Miller and Blackwell, 1992) of a coarse-grained, peralkaline, high-K mafic pluton. The pluton is interpreted to be a strongly differentiated intrusive body of minette magma. 'Average minette' is the average of seventy analyses of mafic Dubawnt minette flows and dykes. 'Average Nueltin' is the average of 72 analyses of Nueltin granite, and 'average Hudson' is the average of 80 analyses of Hudson granitoid rocks.

The Enekatcha shonkinites have exceptionally high REE contents due to the presence of cumulate zircon, REE-rich titanite and apatite, and an unidentified REE accessory mineral (Miller and Blackwell, 1992). The shonkinites are also somewhat anomalous for having elevated concentrations of the heaviest REE (Tm, Yb, Lu). The Nueltin granites and Hudson granitoids have distinct negative Eu anomalies (Eu/Eu*), due to fractionation of plagioclase from the former and restitic plagioclase in the source region of the latter. Negative Eu anomalies in the Dubawnt minettes and the bostonites are usually small or nonexistent, with the exception of bostonite J34B. The bostonite dyke has strongly fractionated REE, with 100Dy/Ce = 0.9 (100Dy/Ce $\approx$ 3 for the other analyses except J34B, 100Dy/Ce = 8.7). The carbonate of J37 has a small positive Eu anomaly, and low overall and extremely non-fractionated REE contents.

The Pearce element diagram (Fig. 6b) shows that the bostonites have signatures common to other Dubawnt minettes, i.e. enrichment in K, Ba, and Th and strong depletions in high field-strength elements (HFSE) such as Nb, P, and Ti. These are indicative of a source region affected by subduction-related metasomatism but importantly, this signature is shared by the granitic suites and therefore must be viewed as a widespread characteristic of the middle to upper crust in the region (e.g. Peterson et al., 2010).

INTERPRETATION AND DISCUSSION

We cannot entirely rule out a late hydrothermal origin for the U- and REE-enriched carbonate at occurrence J34A. Hudson granites, which constitute the outcrop hosting the occurrence, are strongly enriched in U (ca. 50 ppm) relative to most older basement crystalline rocks, and contain zircons with inherited, metamict cores which could yield U if altered further. However, to our knowledge no such alteration veins have been recorded in association with Hudson granites, despite their widespread occurrence. A compilation of U data for Hudson granitoids, Nueltin granites, and Dubawnt minettes (Scott et al., unpub. data) indicates that highly enriched occurrences (3× or more than average) within Hudson plutons are rare, whereas they are commonly recorded in Nueltin granites and Dubawnt minettes.

We prefer an interpretation of an igneous origin (carbonatite) for multiple reasons. The carbonate is closely associated with the microsyenite, which is clearly a strongly differentiated composition. No primary igneous minerals (e.g. feldspar) in the syenitic portion are replaced by carbonate, indicating chemical equilibrium between melt and carbonate minerals. The carbonate is in the central portion of the syenite dyke where more differentiated melt would be expected to accumulate, and the carbonate is rich in euhedral apatite. Similarly, the presence of tabular, idiomorphic crystals of calcite in the J37 occurrence is more consistent with an igneous origin.

Table 2. Analyses of selected samples.

	J34A00*	J34A01*	J34A02*	J34A03*	J34A04*	J34B	J37A2b	J37A2a	J45
Rock	B/C	B/C	B/C	B/C	B/C	B	C	C	B
SiO_2	NA	NA	NA	NA	NA	NA	NA	NA	67.60
TiO_2	0.60	0.63	0.63	0.63	0.57	0.40	0.10	1.25	0.85
Al_2O3	13.49	13.34	9.94	10.96	9.24	12.00	3.48	13.19	14.99
Fe_2O3t	7.82	7.42	5.02	6.85	5.50	3.99	2.37	10.68	3.03
MnO	0.18	0.15	0.09	0.10	0.13	0.05	0.07	0.15	0.02
MgO	6.50	5.87	3.98	4.61	4.11	2.50	0.78	6.53	1.37
CaO	8.54	5.37	2.38	2.06	7.23	3.48	47.85	14.27	0.30
Na_2O	5.45	5.45	2.75	5.69	3.40	1.86	0.09	3.71	0.07
K_2O	0.36	0.36	3.49	0.24	2.65	4.58	0.12	0.24	7.90
P_2O5	0.53	0.56	0.55	0.60	0.54	0.12	0.02	0.12	0.27
H_2O	NA	NA	NA	NA	NA	NA	NA	NA	2.53
S	0.1	BD	0.2	BD	BD	BD	BD	0.1	NA
F	820	840	780	830	810	1540	110	320	466
Cl	BD	BD	180	BD	170	BD	230	BD	NA
Sum	43.56	39.16	29.03	31.74	33.37	28.99	54.89	50.24	99.10
Rb	4.3	7.9	174.5	9.1	127.0	154.5	3.5	2.9	290.6
Cs	0.4	0.4	3.2	0.8	2.1	5.7	0.3	0.4	4.5
Be	10	BD	BD	BD	BD	BD	BD	BD	3
Sr	307	272	656	278	682	72	799	386	134
Ba	39	60	1780	60	1200	650	21	21	1486
Sc	10	10	10	10	10	10	BD	40	BD
Y	84.4	13.9	14.5	12.4	14.5	31.6	6.5	19.3	13.3
Zr	169	190	180	197	167	163	11	77	448
Hf	4.4	5.0	4.6	5.1	4.4	4.4	0.3	2.2	11.6
V	170	130	90	120	100	70	80	190	59
Nb	10.5	9.9	9.6	10.6	9.4	10.2	0.6	5.3	15.3
Ta	0.7	0.7	0.6	0.7	0.6	1.0	BD	0.3	1.1
Cr	70	80	80	90	70	60	20	240	NA
Mo	4	BD	BD	BD	BD	3	BD	BD	0
W	8	6	3	4	3	4	1	3	2
Co	20	20	20	20	20	10	20	50	11
Ni	50	30	20	50	30	30	9	60	15
Cu	450	10	11	10	10	20	270	880	14
Zn	244	125	106	110	94	40	12	94	82
Ga	21.8	24.4	18.8	23.0	19.6	17.2	7.1	15.6	18.6
Tl	BD	BD	1.1	BD	0.8	0.5	BD	BD	0.1
Sn	2	2	2	2	2	3	BD	1	2
Pb	2440	15	20	18	20	70	90	140	2.5
La	108.5	45.5	42.1	64.9	49.8	35.3	4.6	11.3	125.3
Ce	265.0	87.9	87.2	120.5	95.9	67.6	8.1	21.5	245.6
Pr	40.60	11.00	11.50	15.00	11.95	8.51	1.07	2.96	24.51
Nd	160.5	36.9	41.0	51.0	43.5	33.8	4.5	12.9	80.1
Sm	28.00	6.41	7.68	8.10	7.79	8.43	0.97	3.37	9.20
Eu	10.50	1.49	2.15	1.62	1.96	1.65	0.52	1.81	1.94
Gd	24.20	5.48	5.96	6.31	6.21	7.33	1.09	3.72	5.69
Tb	2.56	0.64	0.75	0.69	0.72	1.15	0.17	0.63	0.56
Dy	10.20	2.87	3.23	2.69	3.03	5.89	0.91	3.68	2.19
Ho	1.86	0.55	0.58	0.51	0.57	1.10	0.19	0.74	0.32
Er	5.58	1.76	1.86	1.63	1.71	3.34	0.56	2.28	0.74
Tm	0.57	0.22	0.21	0.20	0.21	0.44	0.06	0.30	0.10
Yb	3.56	1.47	1.50	1.29	1.38	2.52	0.41	1.92	0.52
Lu	0.52	0.23	0.22	0.19	0.21	0.35	0.07	0.27	0.07
Th	15.60	14.40	13.45	14.90	13.45	22.10	0.33	0.87	30.90
U	5740	16.4	14.4	11.8	11.3	350	300	420	17.1

*J34A00 through J34A04 are approximately 5 g aliquots from various parts of sample J34A.
B-bostonite, C-carbonatite, B/C-mixed bostonite/carbonatite
NA-not analyzed, BD-below detection limit
Major elements in wt%, trace elements in ppm

Despite the anomalous radioactivity of the J37 carbonate dyke, it has very low concentrations of incompatible elements (IE), particularly REE. However its field relations, high U and U/Th values, similarities between carbonate and Fe-chlorite bands to J34A and ubiquitous monazite in the chlorite band, support our interpretation that J37 is equivalent to the carbonate portion of J34A. We speculate that the J37 dyke, which contains a very large volume fraction of carbonate, may have further differentiated in situ and that IE-bearing phases were not incorporated in the portions we analyzed. Importantly, we note that the high U/Th values of J34A00 (U/Th = 368) and J37 (U/Th = 696) are not typical of average minette (U/Th = 0.23) or of the strongly differentiated Enekatcha rocks (U/Th = 0.27) and were not observed in the carbonate-free bostonite dyke J45 (U/Th = 0.55) or the J34B bostonite boulder near J34A (U/Th = 16). The U/Th values are seemingly consistent within carbonate-free Dubawnt minettes and not significantly influenced by differentiation. The observed high U/Th values in the carbonate portions of J34A and J37 might result from immiscible segregation of

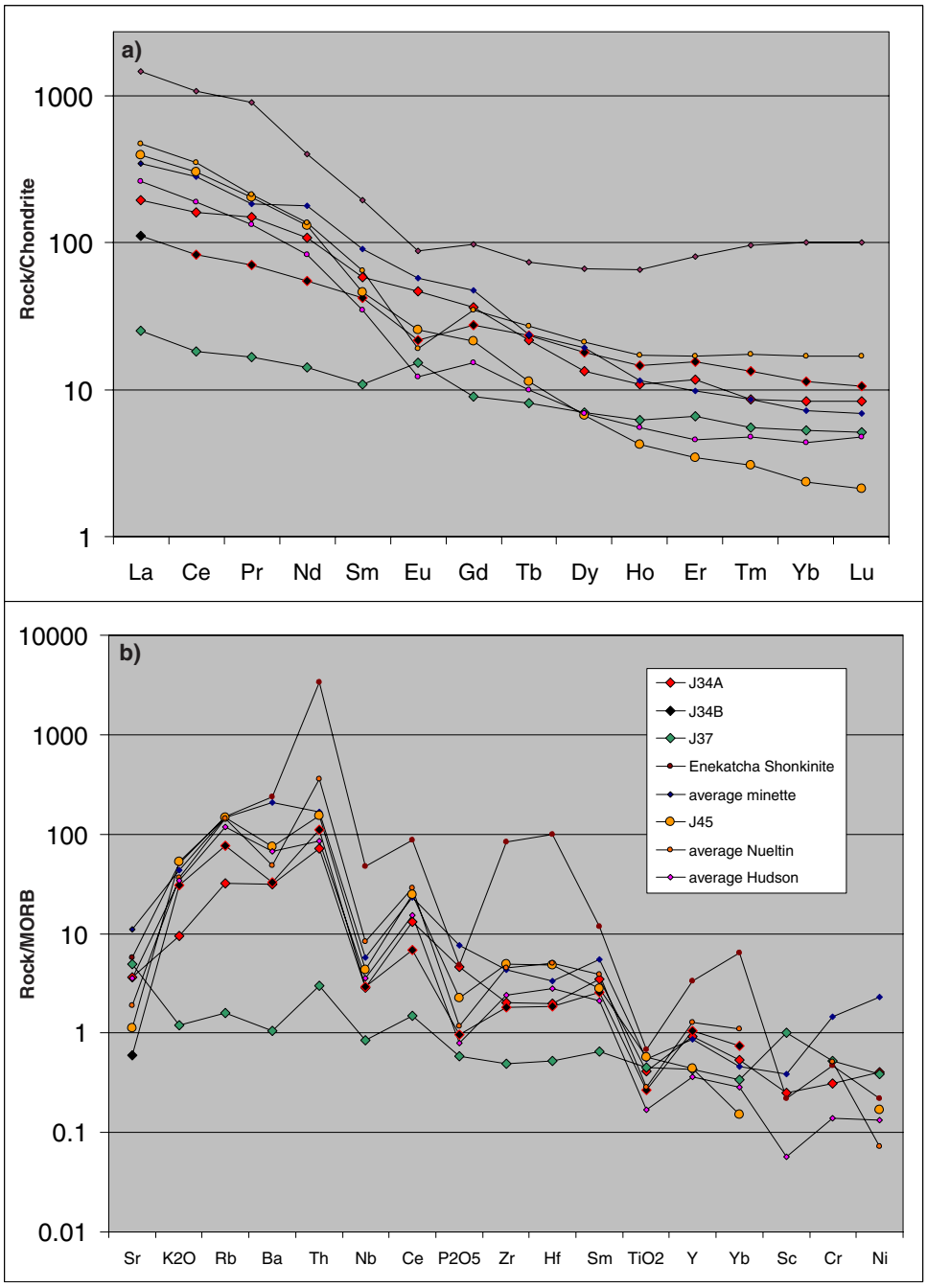

Figure 6. a) REE profiles (rock/chondrite) for the analyzed samples and other igneous rocks of the Dubawnt Supergroup (legend as in 6b). **b)** Pearce diagram (rock/MORB) for the same rocks. *See* text for details.

carbonate melt from silicate magma. Additional outcrops of bostonite dykes in the area will need to be studied to resolve this.

Primary carbonate within the Dubawnt minettes has been previously noted, e.g. it is present in deformed phlogopite megacrysts, interpreted as pieces of the source region of the minettes (Peterson and LeCheminant, 1993). It is therefore not surprising that CO_2 could reach significant concentrations in differentiated magmas of Dubawnt minette, and result in formation of immiscible carbonate magma. A pluton of Dubawnt minette near Judge Sissons Lake (*see* Figure 1, Table 1) sampled by one of us (Jefferson), contains carbonate segregations with idiomorphic crystals of a Ca-LREE fluorocarbonate, tentatively identified as roentgenite-(Ce) (Fig. 7). This pluton, with the property name Nutaaq, is currently being explored for its REE potential, although the highest REE concentrations are in strongly oxidized and altered zones associated with younger brittle faults.

Carbonatites are associated with syenites and ultrapotassic lamprophyres similar to the Dubawnt minettes in the western Yangtze Craton (Tibetan plateau) (Hou et al., 2006). The Tibetan Plateau is a close modern analogue for the western Churchill Province during Dubawnt times (1.85–1.55 Ga), and contains Cenozoic ultrapotassic rocks very similar to the Dubawnt minettes (Peterson et al., 2010 and references therein). The Yangtze carbonatites are unusual for depletions in HFSE and for strongly negative epsilon (Nd) values, both atypical of carbonatites, but characteristics they share with the Dubawnt minettes. One of the three suites described (Dalucao) is REE-enriched and has average $(U/Th)_{carbonatite}/(U/Th)_{syenite}$ of 3.2.

There is insufficient data at this time to attempt correlations of the bostonite dykes with extrusive rocks within the Christopher Island Formation, which contains three regionally identified members of contrasting composition. The youngest (upper felsic minettes) are strongly differentiated felsite lavas, enriched in REE-U-Th, and have some characteristics of lamproites (Peterson, 2006); they are logical candidates to correlate with the bostonites, which may be more widespread than currently recognized. Within the area of the Amer Fault Zone, these typically were emplaced as thin, weakly magnetic dykes trending about 140°. They represent a rich background source of uranium, thorium and REE that may have been further concentrated in more evolved portions of larger intrusive complexes. Such uranium would also have contributed to the supply available for the formation of unconformity-related uranium, in particular by the transport and diagenetic/hydrothermal alteration of non-refractory host minerals such as apatite and monazite (Davis et al., 2011, Jefferson et al., 2007; Mwenifumbo and Bernius, 2007; Mwenifumbo et al., 2007).

We would not be breaking ground to suggest that plutons of the Dubawnt minette suite are prospective for uranium, REE, and associated elements. However, our observations here may indicate that carbonatitic portions of such plutons would be particularly significant. As these are invariably recessively weathered, and boulders would be quickly reduced to small fragments during glacial transport, indirect exploration techniques would be required. We note that iron-rich phases (magnetite, hematite, and chlorite) are likely to be prominent, as is apatite, which indicates that magnetic anomalies and high concentrations of phosphorus may be exploration vectors.

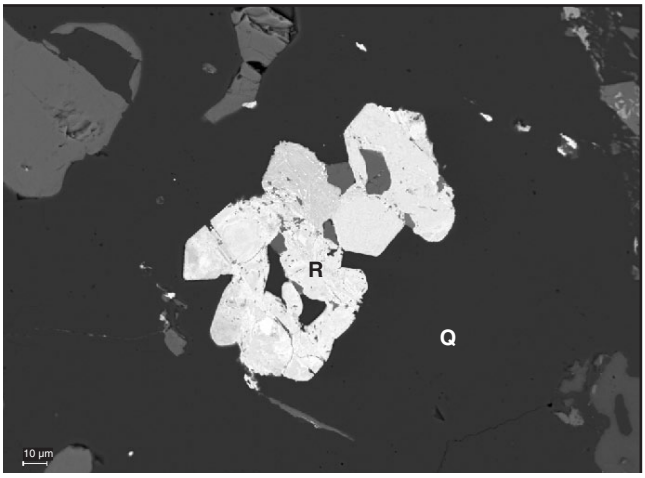

Figure 7. Idiomorphic (hexagonal, bipyramidal) REE fluorocarbonate, Judge Sissons pluton. R = roentgenite-(Ce); Q = quartz. Grey, cleaved mineral in upper left is fluorite. Photograph by P. Hunt. 2011-029

ACKNOWLEDGMENTS

We thank Pat Hunt for her very capable assistance with the SEM study. Helicopter support was provided by Ookpik Aviation under contract to Polar Continental Shelf Program, and by Forrest Helicopters through logistical collaboration with Forum Uranium Corporation. All logistical and analytical costs were covered by the Geomapping for Energy and Minerals Program.

REFERENCES

Davis, W.J., Gall, Q., Jefferson, C.W., and Rainbird, R.H., 2011. Fluorapatite in the Paleoproterozoic Thelon Basin: structural-stratigraphic context, in situ ion microprobe U-Pb ages, and fluid-flow history; Bulletin of the Geological Society of America, v. 123, no. 5/6, p. 1056–1073. doi: 10.1130/B30163.1

Hou, Z., Shihong, T., Zhongxin, Y., Yuling, X., Shuping, Y., Longsheng, Y., Hongcai, F., and Zhiming, Y., 2006. The Himalayan collision zone carbonatites in western Sichuan, SW China: Petrogenesis, mantle source and tectonic implication; Earth and Planetary Science Letters, v. 244, p. 234–250. doi:10.1016/j.epsl.2006.01.052

Jefferson, C.W., Thomas, D.J., Gandhi, S.S., Ramaekers, P., Delaney, G., Brisbin, D., Cutts, C., Portella, P., and Olson, R.A., 2007. Unconformity-associated uranium deposits of the Athabasca Basin, Saskatchewan and Alberta; *in* EXTECH IV: Geology and Uranium EXploration TECHnology of the Proterozoic Athabasca Basin, Saskatchewan and Alberta, (ed.) C.W. Jefferson and G. Delaney; Geological Survey of Canada, Bulletin 588 (also Saskatchewan Geological Society, Special Publication 18; Geological Association of Canada, Mineral Deposits Division, Special Publication 4), p. 23–68. doi:10.4095/223742

LeCheminant, A.N., Miller, A.R., and LeCheminant, G.M., 1987. Early Proterozoic alkaline igneous rocks, District of Keewatin, Canada: petrogenesis and mineralization; *in* Geochemistry and mineralization of Proterozoic volcanic suites, (ed.) T.C. Pharaoh, R.D. Beekinsdale, and D. Rickard; Geological Society Special Publication 33, p. 219–240.

Miller, A.R., 1979. Uranium geology in the central Baker Lake basin, District of Keewatin; *in* Current Research, Part A; Geological Survey of Canada, Paper 79–1A, p. 57–59.

Miller, A.R., 1980. Uranium geology of the eastern Baker Lake basin, District of Keewatin, Northwest Territories; Geological Survey of Canada, Bulletin 330, 63 p.

Miller, A.R. and Blackwell, G.W., 1992. Petrology of alkaline rare earth element bearing plutonic rocks, Enekatcha Lake (65 E/15) and Carey Lake (65 L/7) map-areas. District of Mackenzie; *in* Project Summaries: Canada – Northwest Territories Mineral Development Subsidiary Agreement, 1987–1991, (ed.) D.G. Richardson and D.G. Irving; Geological Survey of Canada, Open File 2484, p. 129–134. doi:10.4095/133305

Mwenifumbo, C.J. and Bernius, G.R., 2007. Crandallite-group minerals: host of thorium enrichment in the eastern Athabasca Basin, Saskatchewan; *in* EXTECH IV: Geology and Uranium EXploration TECHnology of the Proterozoic Athabasca Basin, Saskatchewan and Alberta, (ed.) C.W. Jefferson and G. Delaney; Geological Survey of Canada, Bulletin 588, p. 521–534. doi:10.4095/223742

Mwenifumbo, C.J., Percival, J.B., Bernius, G.R., Elliott, B., Jefferson, C.W., Wasyliuk, K., and Drever, G., 2007. Comparison of geophysical, mineralogical, and stratigraphic attributes in drillholes MAC-218 and RL-88, McArthur River uranium camp, Athabasca Basin, Saskatchewan; *in* EXTECH IV: Geology and Uranium EXploration TECHnology of the Proterozoic Athabasca Basin, Saskatchewan and Alberta, (ed.) C.W. Jefferson and G. Delaney; Geological Survey of Canada, Bulletin 588, p. 521–534. doi:10.4095/223742

Peterson, T.D., 2006. Geology of the Dubawnt Lake area, Nunavut-Northwest Territories; Geological Survey of Canada, Bulletin 580, 56 p. doi:10.4095/221939

Peterson, T.D. and LeCheminant, A.N., 1993. Glimmerite xenoliths in Early Proterozoic ultrapotassic rocks from the Churchill Province; Canadian Mineralogist, v. 31, p. 801–819.

Peterson, T.D., van Breemen, O., Sandeman, H., and Cousens, B., 2002. Proterozoic (1.85–1.75 Ga) igneous suites of the Western Churchill Province: granitoid and ultrapotassic magmatism in a reworked Archean hinterland; Precambrian Research, v. 119, p. 73–100. doi:10.1016/S0301-9268(02)00118-3

Peterson, T.D., Pehrsson, S., Jefferson, C., and Scott, J., 2010. The Dubawnt Supergroup, Canada: a LIP with a LISP; International Association of Volcanology and Chemistry of the Earth's Interior: Large Igneous Provinces Commission; LIP of the Month, December 2010; International Association of Volcanology and Chemistry of the Earth's Interior, <http://www.largeigneousprovinces.org/10dec> [accessed June 23, 2010].

Tella, S., 1994. Geology, Amer Lake (66 H), Deep Rose Lake (66 G) and parts of Pelly Lake (66 F); Geological Survey of Canada, Open File 2969, scale 1:250 000. doi:10.4095/194789

Tella, S., Ashton, K.E., Thompson, D.L., and Miller, A.R., 1983. Geology of the Deep Rose Lake map area, District of Keewatin; *in* Current Research, Part A; Geological Survey of Canada, Paper 83–01A, p. 403–409.

Tella, S., Heywood, W.W., and Loveridge, W.D., 1985. A U-Pb age on zircon from a quartz syenite intrusion, Amer Lake map area, District of Keewatin; *in* Current Research, Part B; Geological Survey of Canada, Paper 85-1B, p 367–370.

van Breemen, O., Peterson, T.D., and Sandeman, H.A., 2005. U-Pb geochronology and Nd isotope geochemistry of Proterozoic granitoids in the Western Churchill Province: intrusive age pattern and Archean source domains; Canadian Journal of Earth Sciences, v. 42, p. 339–377. doi:10.1139/e05-007

Geologcial Survey of Canada Project # EGM007